Available online at www.sciencedirect.com
SCIENCE DIRECT®
Biomaterials 25 (2004) 4731–4739
Biomaterials
www.elsevier.com/locate/biomaterials

Increased osteoblast adhesion on nanophase metals: Ti, Ti6Al4V, and CoCrMo

Thomas J. Webster*, Jeremiah U. Ejiofor

Department of Biomedical Engineering, Purdue University, 1296 Patter Building, West Lafayette, IN 47905, USA

Received 9 October 2003; accepted 2 December 2003

Abstract

Previous studies have demonstrated increased functions of osteoblasts (bone-forming cells) on nanophase compared to conventional ceramics (specifically, alumina, titania, and hydroxyapatite), polymers (such as poly lactic-glycolic acid and polyurethane), carbon nanofibers/nanotubes, and composites thereof. Nanophase materials are unique materials that simulate dimensions of constituent components of bone since they possess particle or grain sizes less than 100 nm. However, to date, interactions of osteoblasts on nanophase compared to conventional metals remain to be elucidated. For this reason, the objective of the present in vitro study was to synthesize, characterize, and evaluate osteoblast adhesion on nanophase metals (specifically, Ti, Ti6Al4V, and CoCrMo alloys). Such metals in conventional form are widely used in orthopedic applications. Results of this study provided the first evidence of increased osteoblast adhesion on nanophase compared to conventional metals. Interestingly, osteoblast adhesion occurred preferentially at surface particle boundaries for both nanophase and conventional metals. Since more particle boundaries are present on the surface of nanophase compared to conventional metals, this may be an explanation for the measured increased osteoblast adhesion. Lastly, material characterization studies revealed that nanometal surfaces possessed similar chemistry and only altered in degree of nanometer surface roughness when compared to their respective conventional counterparts. Because osteoblast adhesion is a necessary prerequisite for subsequent functions (such as deposition of calcium-containing mineral), the present study suggests that nanophase metals should be further considered for orthopedic implant applications.

Keywords: Nanotechnology; Metals; Ti; Ti6Al4V; CoCrMo; Osteoblasts

1. Introduction

For over seven decades, material scientists, orthopedic surgeons, and allied bioengineers have continued to investigate means of eliminating or, at least, reducing the incidence of bone implant failures in humans. Experts in the orthopedic field in part blame the underperformance of these implants on incomplete osseointegration (i.e., lack of bonding of an orthopedic implant to juxtaposed bone) between surrounding bone and the prostheses [1–4]. Others suspect severe stress shielding as responsible [2–4] and attribute the shielding effect to significant differences in mechanical properties between an implant and surrounding bone. Still others implicate the generation of wear debris at articulating surfaces of orthopedic implants that lead to bone cell death and perhaps eventual necrotic bone [3,4]. Clearly, novel materials are needed which address each of the above concerns simultaneously.

A recent approach to the design of the next-generation of orthopedic implants has centered on matching the unique nanometer topography created by natural extracellular matrix proteins found in the bone tissue in synthetic implant surfaces [5–14]. While the nanometer structures and molecules found in bone tissue clearly indicate that bone-forming cells are accustomed to interacting with surfaces of nanometer roughness, conventional synthetic metals currently applied in the clinics exhibit micro-rough surfaces and are smooth at the nanoscale [3,4]. For instance, woven (or immature) bone has an average inorganic mineral grain size of 10–50 nm [4]. Lamellar bone, which actively replaces woven bone, has an average inorganic mineral grain size of 20–50 nm long and is 2–5 nm in diameter [4]. But at nanoscale dimensions, many, if not all, currently utilized implant surfaces are smooth [3,4].

*Corresponding author. Tel.: +1-765-494-2995; fax: +1-765-494-1193.
E-mail address: twebster@ecn.purdue.edu (T.J. Webster).

0142-9612/$ - see front matter © 2003 Elsevier Ltd. All rights reserved.
doi:10.1016/j.biomaterials.2003.12.002

Such smooth surfaces have been shown to favor "fibrointegration," (callus formation) which can, ultimately, encapsulate implants placed in bone with stratified undesirable connective tissue [3,4].

Indeed, several studies have positively correlated the adhesion and functions of bone cells with the nanoscale surface features of potential implants [5–14]. For instance, compared to conventional (micron-size) ceramic formulations, nanostructured substrates made separately from spherical particles of alumina (Fig. 1), titania, and hydroxyapatite enhanced adhesion of osteoblasts (bone-forming cells), decreased adhesion of fibroblasts (cells that contribute to fibrous encapsulation and callus formation events that may lead to implant loosening and failure), and decreased adhesion of endothelial cells (cells that line the vasculature of the body) [7]. In fact, calcium deposition by osteoblasts was four, three, and two times greater on nanophase compared to conventional alumina, titania, and hydroxyapatite after 28 days of culture, respectively [11]. Compared to respective conventional counterparts, comparative studies have also demonstrated increased calcium deposition by osteoblasts cultured on alumina nanofibers, carbon nanofibers, poly-lactic-glycolic acid, polyurethane, and composites thereof [8–10,12]. In each of the studies, chemistry was similar between nanophase and conventional comparisons and the inherent increase in surface area of nanophase materials was taken into account [7–12].

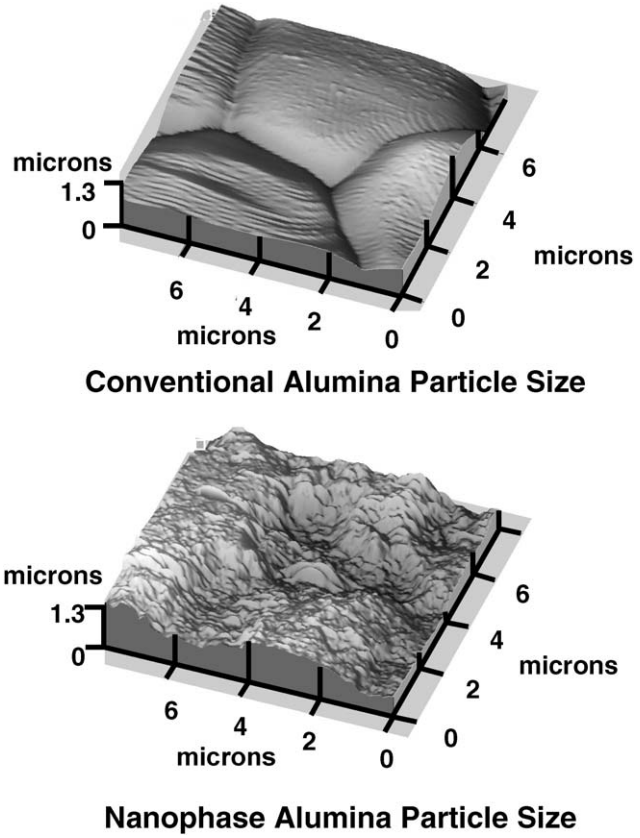

Fig. 1. Atomic force micrographs of nanophase compared to conventional alumina. Previous studies have demonstrated increased select functions of osteoblasts on nanometer particle size ceramics such as alumina, titania, and hydroxyapatite.

However, one material classification is missing from this growing list of nanophase materials that promote functions of osteoblasts: metals. For this reason, the objective of this in vitro study was to determine osteoblast adhesion on nanophase compared to conventional Ti, Ti6Al4V, and CoCrMo alloys. To the best of our knowledge this is the first study to evaluate osteoblast function on nanophase compared to conventional metals that have similar chemistry and alter only in degree of nanometer surface roughness.

2. Materials and methods

2.1. Materials selection and synthesis of compacts

The objective of the material synthesis phase was to generate nanostructured surface features for metals that are currently in use as orthopedic implants. Concerns of surface chemistry alterations—a possible effect of exposing fine particulates of reactive metals to unprotective, oxidizing, or contaminated atmospheres at elevated temperatures—were avoided by creating powder metallurgy compacts in the absence of heat [13]. Powders of metals and alloys currently in clinical use for orthopedic purposes were studied [3,4]. Specific interest was directed on those materials that are designed for processing via powder metallurgy techniques.

These materials included commercially pure titanium (c.p. Ti), Ti6Al4V ELI, and Co28Cr6Mo. Powders were obtained from Powder Tech Associates (Bedford, MA). Details for each category of metal particulates are provided in Table 1. Nanophase and conventional particle sizes in each respective metal category (Ti, Ti6Al4V, and CoCrMo) were obtained. Each respective group of nanophase and conventional particulates possessed the same material properties (chemistry and shape) and altered only in dimension.

Powders were loaded into a steel-tool die to obtain compacts for use in cell experiments. One pressure level (10 GPa over 5 min) was used to press all Ti-based compacts to green densities 90–95% of theoretical. At a different pressure level (5 GPa over 5 min), particles of the CoCr-based elemental blends were pressed. All pressed green discs (diameter: 12 mm, thickness: 0.50–1.10 mm) were produced using a simple uniaxial, single-ended compacting hydraulic press (Carver, Inc). Powders were pressed in air at room temperature.

Rolled, heat-treated, and pickled c.p. Ti sheets (wrought Ti; Osteonics) were used as controls during the cell experiments. Borosilicate glass (Fisher) etched in

Table 1
Metal particles[a]

Material	Type	ASTM designation	Particle size (μm)	Particle shape
Ti	Nano	F-67; G2	0.5–2.4	Spongy
Ti	Conv	F-67; G2	>10.5	Spongy
Ti6A14V (prealloyed)	Nano	F-136	0.5–1.4	Spongy (Ti); irregular (Al/V)
Ti6A14V (prealloyed)	Conv	F-136	>7.5	Spongy (Ti); irregular (Al/V)
Co28Cr6Mo (blend elemental)	Nano	F-75; F-799	0.2–0.4	Spherical (Co); irregular (Cr and Mo)
Co28Cr6Mo (blend elemental)	Conv	F-75; F-799	44–106	Spherical (Co); irregular (Cr and Mo)

[a] Metal particle with dimensions less than and greater than 1 μm were given the classification of nanophase (abbreviated "nano") and conventional (abbreviated "conv"), respectively.

10 N NaOH for 1 h was also utilized as a reference substrate in the cell experiments. All substrates were sterilized by UV exposure for 1 h on each side.

2.2. Surface characterization

The surfaces of the metal compacts were characterized for roughness using scanning electron microscopy (SEM) and atomic force microscopy (AFM). For SEM, substrates were first sputter-coated with a thin layer of gold-palladium using a Hummer I Sputter Coater (Technics) in a 100 mTorr vacuum argon environment for a 3 min period and 10 mA of current. Images were taken using a JEOL JSM-840 Scanning Electron Microscope at a 5 kV accelerating voltage. Digital images were recorded using the Digital Scan Generator Plus (JEOL) software. For wrought Ti (reference), samples were also treated in an acidified ($HF + HNO_3$) aqueous environment to reveal grain sizes; images of the wrought Ti control were obtained using both SEM and an optical microscope (Leica).

For AFM, a NanoScope IIIa Atomic Force Microscope with NanoScope imaging software (Digital Instruments, Inc.) was used to quantify surface roughness. A scan rate of 2 Hz and 512 scanning points were used to obtain root-mean-square roughness values. All scans were performed in ambient air (at 15–20% humidity). Experiments were completed in triplicate at three separate times.

2.3. Cell experiments

Human osteoblasts (bone-forming cells; CRL-11372 American Type Culture Collection, population numbers 6–8) in Dulbecco's Modified Eagle Medium (Gibco) supplemented with 10% fetal bovine serum (Hyclone) and 1% Penicillin/Streptomycin (Hyclone) were seeded at a density of 3500 cells/cm^2 onto the substrates of interest and were then placed in standard cell culture conditions (that is, a humidified, 5% CO_2/95% air environment) for either 1 or 3 h. After the prescribed time period, substrates were rinsed in phosphate buffered saline to remove any non-adherent cells. The remaining cells were fixed with formaldehyde, stained with Hoescht 33258 dye (Sigma), and counted under a fluorescent microscope (Leica). Five random fields were counted per substrate. All experiments were run in triplicate and repeated at least three separate times. Numerical data was analyzed using standard analysis of variance (ANOVA) followed by Duncan's multiple range tests.

Osteoblast morphology and adhesion location on the substrates of interest was examined using SEM. At the end of the prescribed time period, cells were dehydrated through sequential washings in 50%, 60%, 70%, 80%, and 90% ethanol (remainder deionized water) solutions. Samples were then critically point dried according to standard techniques [7]. Lastly, samples were sputter-coated with a thin layer of gold-palladium using a Hummer I Sputter Coater (Technics) in a 100 mTorr vacuum argon environment for 3 min and 10 mA of current. Similar to samples without cells, images were taken using a JEOL JSM-840 scanning electron microscope at a 5 kV accelerating voltage. Digital images were recorded using the Digital Scan Generator Plus (JEOL) software.

3. Results

3.1. Surface characterization

Results provided evidence of increased nanometer surface roughness in nanophase compared to conventional Ti (Fig. 2), Ti6Al4V (Fig. 3), and CoCrMo (Fig. 4). As expected, the dimensions of nanometer surface features gave rise to larger amounts of interparticulate voids (with fairly homogeneous distribution) in nanophase Ti and Ti6Al4V, unlike the corresponding conventional Ti and Ti6Al4V compacts; these latter compacts rather revealed less amounts of interparticulate voids with a non-homogeneous distribution.

As appeared in Table 1, spherical (Co) and irregular (Cr and Mo) powder particle elemental blends were

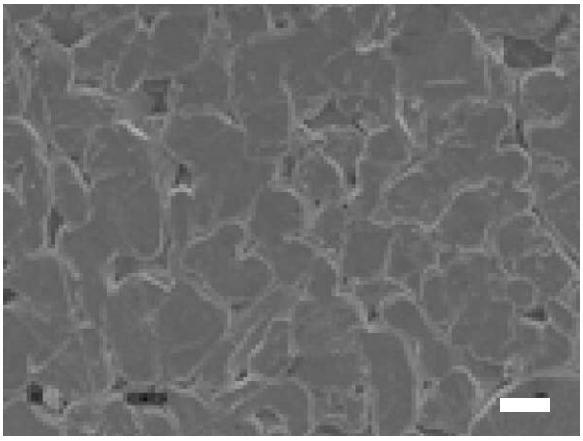

Nanophase
Ti

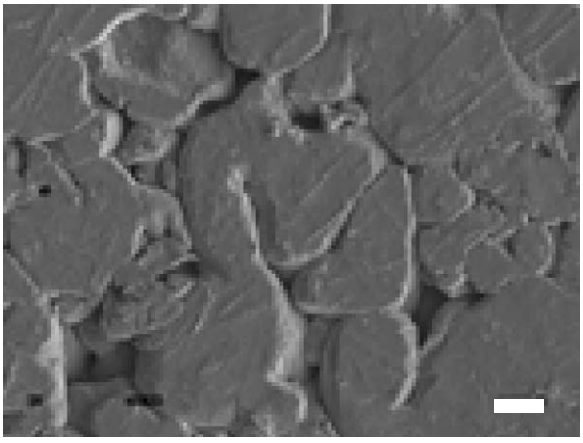

Conventional
Ti

Fig. 2. Scanning electron microscopy images of Ti compacts. Increased nanostructured surface roughness was observed on nanophase compared to conventional Ti. Bar = 1 μm for nanophase Ti and 10 μm for conventional Ti.

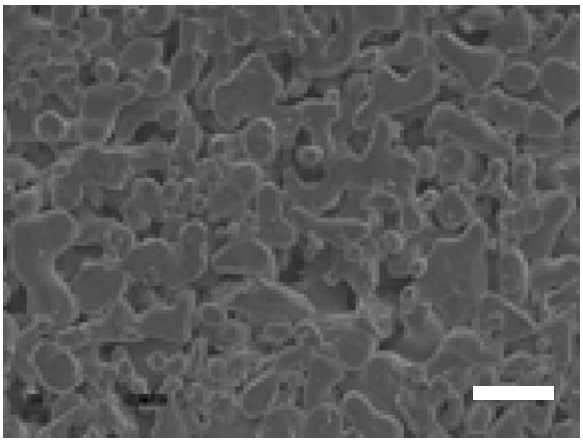

Nanophase
Ti6Al4V

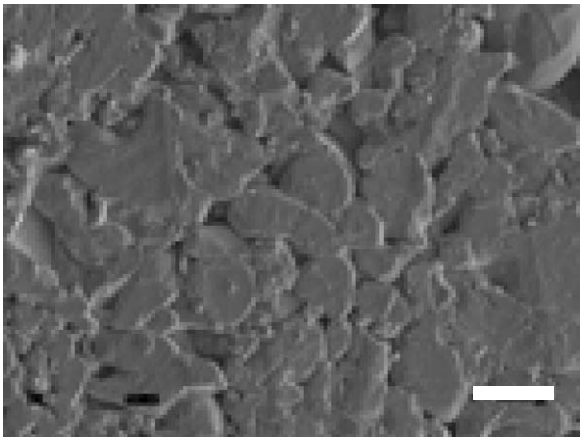

Conventional
Ti6Al4V

Fig. 3. Scanning electron microscopy images of Ti6Al4V compacts. Increased nanostructured surface roughness was observed on nanophase compared to conventional Ti6Al4V. Bar = 1 μm for nanophase Ti6Al4V and 10 μm for conventional Ti6Al4V.

pressed into nanophase CoCrMo (made from nanometer particle sizes: 0.2–0.4 μm) and into conventional CoCrMo (made from large micron particle sizes: 44–106 μm). Unlike conventional CoCrMo compacts, high interparticulate void density (number of voids per unit area) and nanometer void sizes (less than 1 μm) were exhibited on nanophase CoCrMo (Fig. 4). Few relatively large particles can be seen with cleavage-like facets in nanophase CoCrMo. The substrates made out of coarse particles (conventional CoCrMo), in contrast, appeared only minimally deformed. The deformed particle size is within the 50–160 μm range. Interparticulate voids were large (10–50 μm) and void density was small for the conventional CoCrMo compacts.

The exposed topography of the wrought Ti sheet (reference substrate; Fig. 5) showed surface features in the range 20–60 μm. Moreover, after etching in an acidic ($HF + HNO_3$) aqueous solution, wrought Ti showed grain sizes in the traditional range of 20–50 μm (roughly equivalent to ASTM No. 7.5) under optical microscopy (Fig. 5).

Atomic force microscopy data confirmed the increased nanometer surface roughness of the nanophase compared to conventional metals (Table 2). Specifically, 2.4, 3.1, and 1.9 times the amount of nanometer surface roughness was measured on nanophase compared to conventional Ti, Ti6Al4V, and CoCrMo substrates. Due to this increase in surface roughness, increased surface area was also measured for the nanophase compared to conventional metals. Specifically, 15%, 23%, and 11% more surface area was measured on nanophase compared to conventional Ti, Ti6Al4V, and CoCrMo compacts.

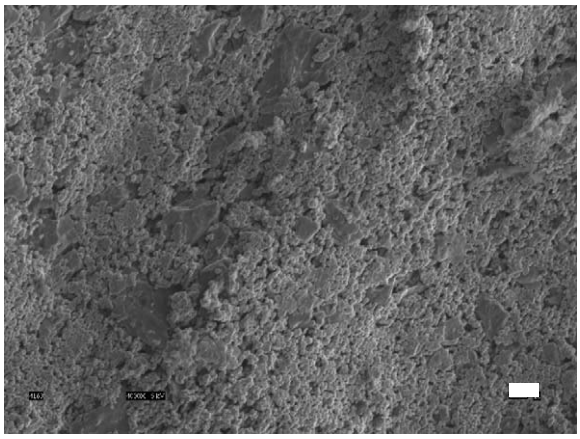

Nanophase CoCrMo

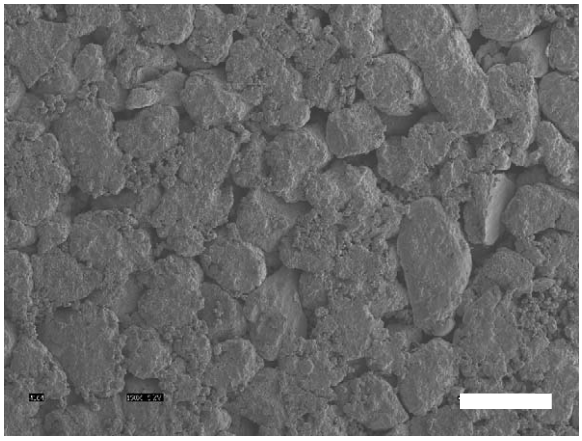

Conventional CoCrMo

Fig. 4. Scanning electron microscopy images of CoCrMo compacts. Increased nanostructured surface roughness was observed on nanophase compared to conventional CoCrMo. Bar = 1 μm for nanophase CoCrMo and 100 μm for conventional CoCrMo.

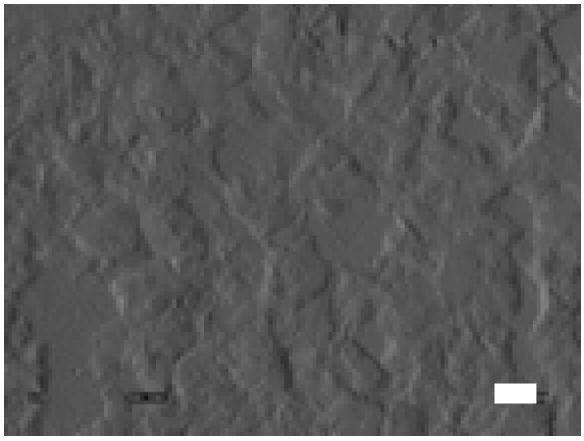

Scanning Electron Microscope Image of Wrought Ti (reference)

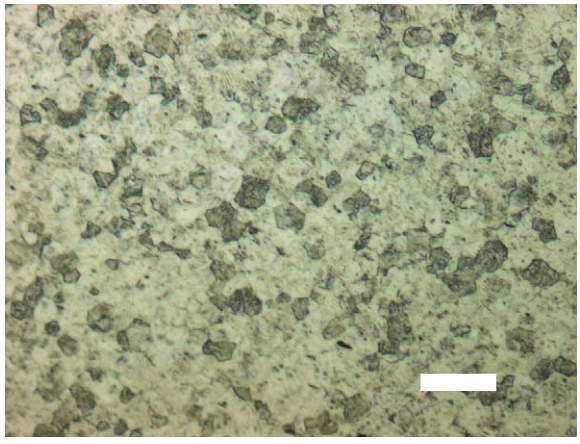

Optical Microscope Image of Wrought Ti Acidic Etched to Reveal Grains (reference)

Fig. 5. Images of wrought Ti (reference). Scanning electron images of wrought Ti indicated a large degree of microsurface roughness. Acidic etching of the wrought Ti samples revealed grain sizes 20–50 μm (roughly equivalent to ASTM No. 7.5) under optical microscopy. Bar = 10 μm for wrought Ti (reference) and 50 μm for wrought Ti acid etched to reveal grains (reference).

3.2. Cell experiments

Results of the present study provided the first evidence of increased osteoblast adhesion on nanophase compared to conventional Ti (Fig. 6), Ti6Al4V (Fig. 6), and CoCrMo (Fig. 7). Specifically, osteoblast adhesion was significantly ($p<0.01$) greater on nanophase Ti when compared to either conventional Ti or wrought Ti (reference) after 1 and 3 h. Similarly, compared to either conventional Ti6Al4V or wrought Ti (reference), osteoblast adhesion was significantly ($p<0.01$) greater on nanophase Ti6Al4V after 1 and 3 h. In contrast, osteoblast adhesion was similar between wrought Ti, conventional Ti, and conventional Ti6Al4V. While osteoblast adhesion increased ($p<0.01$) from 1 to 3 h on wrought Ti and nanophase Ti, it remained the same on all other substrates. Cell adhesion was normalized to the increase in surface area of the nanophase Ti and Ti6Al4V formulations.

Table 2
Surface roughness of metal compacts

Substrate	Surface roughness (rms; nm)
Ti (nano)	11.9
Ti (conv)	4.9
Ti6Al4V (nano)	15.2
Ti6Al4V (conv)	4.9
CoCrMo (nano)	356.7
CoCrMo (conv)	186.7

While osteoblast adhesion was greater ($p<0.01$) on nanophase CoCrMo compared to conventional

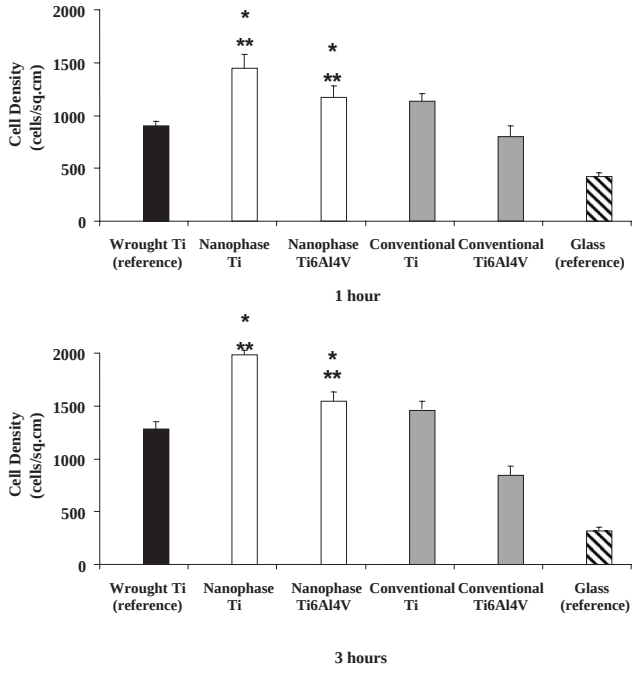

Fig. 6. Increased osteoblast adhesion on nanophase Ti and Ti6Al4V compacts. Data = mean ± SEM; $n = 3$; $^{*}p < 0.01$ compared to respective conventional metal and $^{**}p < 0.01$ compared to wrought Ti (reference).

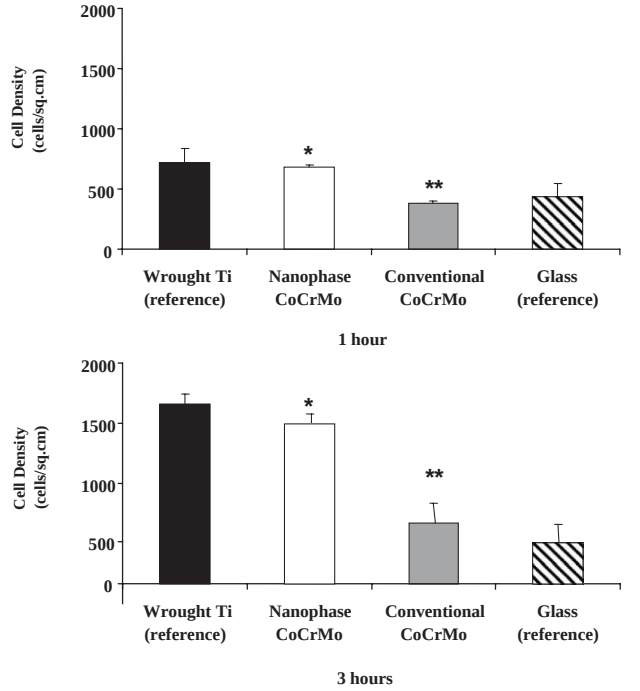

Fig. 7. Increased osteoblast adhesion on nanophase CoCrMo compacts. Data = mean ± SEM; $n = 3$; $^{*}p < 0.01$ compared to respective conventional CoCrMo and $^{**}p < 0.01$ compared to wrought Ti (reference).

CoCrMo, similar osteoblast adhesion was measured between wrought Ti (reference) and nanophase CoCrMo after 1 and 3 h (Fig. 7). Osteoblast adhesion was significantly ($p < 0.01$) less on conventional CoCrMo compared to wrought Ti (reference). While osteoblast adhesion increased ($p < 0.01$) from 1 to 3 h on wrought Ti and nanophase CoCrMo, it remained the same on all other substrates. Cell adhesion was normalized to the increase in surface area of the nanophase CoCrMo formulations.

Interestingly, when analyzing spatial location of cell adhesion on the substrates of interest to the present study, osteoblast adhesion occurred primarily at particle boundaries (Figs. 8 and 9 for Ti and Ti6Al4V, respectively). Since nanophase materials possess increased particle boundaries at the surface (due to smaller particle size), this may be an explanation for the increased osteoblast adhesion measured on nanophase formulations. Lastly, under high magnification images, cell protrusions specifically at particle boundaries are indicated by arrows on the images (Figs. 8 and 9). These are representative images which reflect what was observed over the entire surface.

4. Discussion

For the first time, this manuscript represents an attempt to advance design criteria utilized for improving osteoblast function on ceramics [7,11,14], polymers [9,10], and composites [9,10] to metals. In doing so, the present study adds metals to the growing list of materials [7–14] that when created to possess constituent nanometer particulates, promotes osteoblast adhesion. Since adhesion of osteoblasts is a necessary prerequisite for subsequent functions (such as deposition of calcium containing mineral), this study implies further enhanced functions of osteoblasts on nanophase Ti, Ti6Al4V, and CoCrMo; clearly, however, more studies would be needed to verify this. It is important to note that although this study demonstrated increased osteoblast adhesion on three metals with vastly different chemistries (Ti compared to Ti6Al4V compared to CoCrMo), the same promising net affect resulted. Especially when collectively considering the nanophase ceramic [7,11,14], polymer [9,10], and composite [9,10] systems evaluated to date, the present results provide strong evidence that osteoblast attachment may be promoted regardless of material chemistry as long as a large degree of nanometer surface roughness is created.

It is important to note that the idea of creating metallic implants with decreased surface feature dimensions (i.e. into the nanometer regime) in order to mimic the roughness of extracellular matrices in bone has also been utilized by others [5,6]. However in such studies, the modified synthetic materials varied in a number of properties, not just degree of nanometer surface roughness, that may have also influenced osteoblast function [5]. For example, it has been reported that Ti and

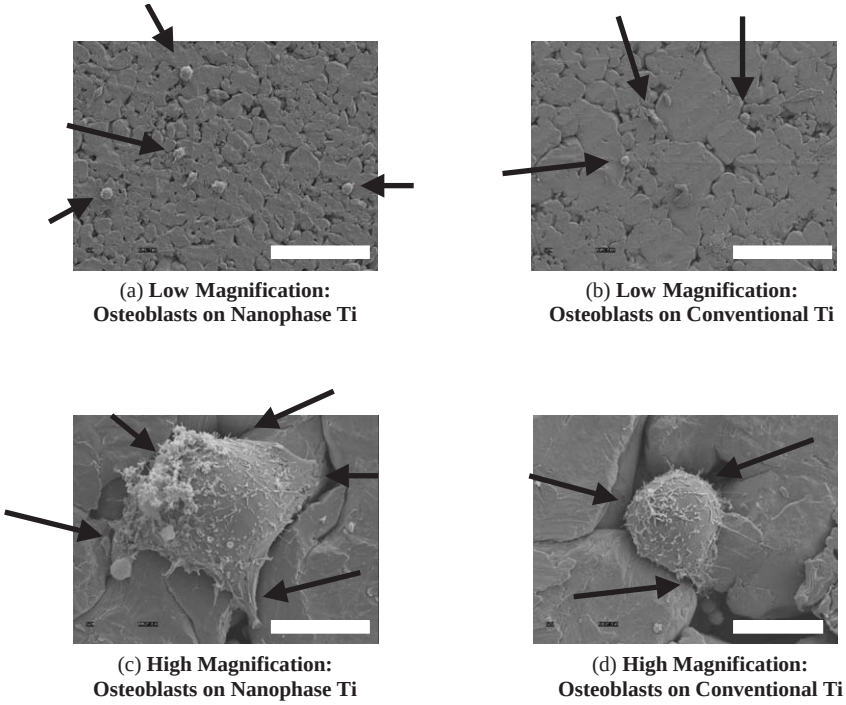

(a) **Low Magnification: Osteoblasts on Nanophase Ti**

(b) **Low Magnification: Osteoblasts on Conventional Ti**

(c) **High Magnification: Osteoblasts on Nanophase Ti**

(d) **High Magnification: Osteoblasts on Conventional Ti**

Fig. 8. Scanning electron microscopy images of osteoblasts on Ti compacts. Osteoblast adhesion was observed at Ti particle boundaries. Since nanophase metals have increased particles boundaries compared to conventional metals, it is speculated that this may be one reason for increased osteoblast adhesion on nanophase metals. Bar = 100 and 10 μm for low and high magnification images, respectively. Arrows indicate cells (low magnification) and area where cell protrusions are seen specifically at particle boundaries (high magnification). Adhesion time = 1 h.

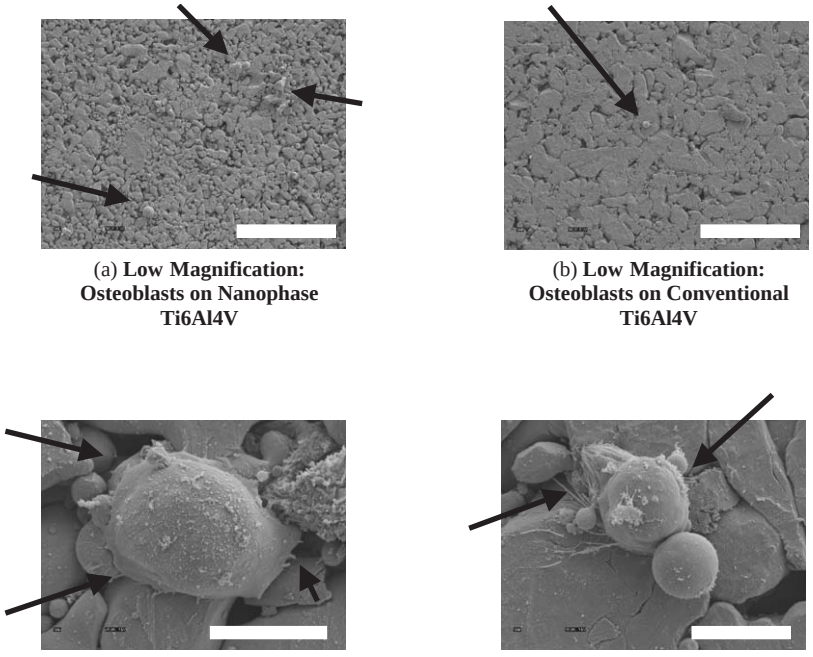

(a) **Low Magnification: Osteoblasts on Nanophase Ti6Al4V**

(b) **Low Magnification: Osteoblasts on Conventional Ti6Al4V**

(c) **High Magnification: Osteoblasts on Nanophase Ti6Al4V**

(d) **High Magnification: Osteoblasts on Conventional Ti6Al4V**

Fig. 9. Scanning electron microscopy images of osteoblasts on Ti6Al4V compacts. Osteoblast adhesion was observed at Ti6Al4V particle boundaries. Since nanophase metals have increased particles boundaries compared to conventional metals, it is speculated that this may be one reason for increased osteoblast adhesion on nanophase metals. Bar = 100 and 10 μm for low and high magnification images, respectively. Arrows indicate cells (low magnification) and area where cell protrusions are seen specifically at particle boundaries (high magnification). Adhesion time = 1 h.

Ti6Al4V treated with H_2SO_4 and H_2O_2 to create nanotextured surfaces promoted osteoblast osteopontin and bone sialoprotein synthesis [5]. Although this represents a novel finding, due to chemistry changes that may have occurred during chemical treatment of Ti and Ti6Al4V, it is not clear which property (chemistry or nanometer roughness) increased functions of osteoblasts. In addition, other efforts to modify surface roughness in metals have included chemical methods like solvent cleaning/pickling [1], alkaline etching [15,16], electropolishing [17], and glow-discharge treatment [18,19]. In all cases, it is unclear what underlying material property is controlling cell function.

This investigation was specifically designed to provide the first evidence of whether nanophase Ti, Ti6Al4V, and CoCrMo alloy formulations influence osteoblast attachment solely due to nanometer surface roughness characteristics. Since metal particulates were chosen with similar respective chemistries and these powders were pressed without the use of heat, the same chemistries were compared between respective nanophase and conventional formulations [13].

Lastly, it is intriguing to ponder why osteoblast adhesion occurred selectively at nanophase metal particle boundaries. Since nanophase metals are composed of particles of the same atoms but fewer (less than tens of thousands) and smaller (less than 100 nm in diameter) than conventional forms (which contain several billions of atoms and have particle sizes microns to millimeters in diameter), nanophase metals have unique surface properties [20]. In this respect, nanophase metals have higher numbers of atoms at the surface compared to bulk, greater areas of increased surface defects (such as edge/corner sites and particle boundaries), and larger proportions of surface electron delocalization [21]. Such altered surface properties will influence initial protein interactions that control subsequent cell adhesion.

In fact, investigations of the underlying mechanisms of increased osteoblast adhesion on nanophase ceramics revealed that the initial adsorbed concentration [22], conformation [23], and bioactivity [23] of proteins contained in serum was responsible. For example, by just decreasing ceramic grain size to below 100 nm, select competitive vitronectin adsorption increased 10% on alumina formulations [22,23]; this may in part have promoted osteoblast adhesion on nanophase alumina. In addition, increased unfolding of vitronectin was measured on nanophase compared to conventional alumina [23]. Increased unfolding of vitronectin promoted the availability of specific cell-adhesive epitopes (such as the amino acid sequence: Arg–Gly–Asp or RGD) to increase osteoblast adhesion [23]. Although experiments would be needed to verify this, the same events of optimal initial protein interactions for osteoblast adhesion may be happening on nanophase metals. This is supported by the fact that osteoblasts were observed to specifically adhere to particle boundaries which contain greater surface reactivity to influence initial protein interactions that control subsequent cell adhesion.

5. Conclusions

The present study provided the first evidence of increased osteoblast adhesion on Ti, Ti6Al4V, and CoCrMo compacts with nanometer compared to conventionally sized particles. Respective metal formulations had similar chemistry and altered only in degree of nanometer roughness. Interestingly, osteoblasts were observed to adhere specifically at particle boundaries. Since nanophase metals have higher percentages of particle boundaries at the surface, this may explain the greater numbers of osteoblasts on nanophase compared to conventional metals. Since adhesion is a necessary prerequisite for subsequent functions of osteoblasts (such as the deposition of calcium-containing mineral), these results suggest for the first time the promise nanophase metals have in orthopedic applications.

Acknowledgements

The authors would like to thank the Whitaker Foundation and the National Science Foundation for funding. We would also like to thank Prof. Albena Ivanisevic for assistance with AFM.

References

[1] Buser D, Nydegger T, Oxland T, Cochran DL, Schenk RK, Hirt HP, Snetivy D, Nolte LP. Interface shear strength of titanium implants with a sanblasted and acid-etched surface: a biomechanical study in the maxilla of miniature pigs. J Biomed Mater Res 1999;45:75.

[2] Webster TJ. Nanophase ceramics: the future of orthopedic and dental implant material. In: Ying JY, editor. Nanostructured materials. New York: Academy Press; 2001. p. 125–66.

[3] Kaplan FS, Hayes WC, Keaveny TM, Boskey A, Einhorn TA, Iannotti JP. Biomaterials. In: Simon SP, editor. Orthopedic basic science. Columbus, OH: American Academy of Orthopedic Surgeons; 1994. p. 460–78.

[4] Kaplan FS, Lee WC, Keaveny TM, Boskey A, Einhorn TA, Iannotti JP. Form and function of bone. In: Simon SP, editor. Orthopedic basic science. Columbus, OH: American Academy of Orthopedic Surgeons; 1994. p. 127–85.

[5] de Oliveira PT, Nanci A. Nanotexturing of titanium-based surfaces upregulates expression of bone sialoprotein and osteopontin by cultured osteogenic cells. Biomaterials 2004;25:403–13.

[6] Kawaguchi H, McKee MD, Okamoto H, Nanci A. Immunocytochemical and lectin-gold characterization of the interface between alveolar bone and implanted hydroxyapatite in the rat. Cells Mater 1993;3:337.

[7] Webster TJ, Siegel RW, Bizios R. Osteoblast adhesion on nanophase ceramics. Biomaterials 1999;20:1221.
[8] Elias KE, Price RL, Webster TJ. Enhanced functions of osteoblasts on nanometer diameter carbon fibers. Biomaterials 2000;23:3279.
[9] Kay S, Thapa A, Haberstroh KM, Webster TJ. Nanostructured polymer/nanophase ceramic composites enhance osteoblast and chondrocyte adhesion. Tissue Eng 2002;8:753.
[10] Price RL, Waid MC, Haberstroh KM, Webster TJ. Increased, select bone cell adhesion on formulations containing carbon nanofibers. Biomaterials 2003;24:1877.
[11] Webster TJ, Siegel RW, Bizios R. Enhanced functions of osteoblasts on nanophase ceramics. Biomaterials 2000;21:1803.
[12] Supronowicz PR, Ajayan PM, Ullmann KR, Arulanandam BP, Metzger DW, Bizios R. Novel current-conducting composite substrates for exposing osteoblasts to alternating current stimulation. J Biomed Mater Res 2002;59:499.
[13] Ejiofor JU, Webster TJ. Topography and morphology effects of titanium bone implant on osteoblasts adhesion in vitro. Presented at the 2003 International Conference on Powder Metallurgy & Particulate Materials. Princeton, NJ: Metal Powder Industries Federation (MPIF), Las Vegas, NV; June 8–12, 2003.
[14] Webster TJ, Siegel RW, Bizios R. Design and evaluation of nanophase alumina for orthopedic/dental applications. Nanostruct Mater 1999;12:983.
[15] Nishiguchi S, Nakamura T, Kobayashi M, Kim HM, Miyaji F, Kokubo T. The effect of heat treatment on bone bonding ability of alkali-treated titanium. Biomaterials 1999;20:49.
[16] Wen HB, Liu Q, de Wijn JR, de Groot K, Cui FZ. Preparation of bioactive microporous titanium surface by a new two-step chemical treatment. J Mater Sci: Mater Med 1998;9:121.
[17] Larsson C, Thomsen P, Aronsson BO, Rodahl M, Lausmaa J, Kasemo B, Ericson LE. Bone response to surface modified titanium implants: studies on electropolished implants with different oxide thicknesses and morphology. Biomaterials 1994;15:1325.
[18] Bordji K, Jouzeau JY, Mainard D, Payan E, Netter P, Rie KT, Stucky T, Hage-Ali M. Cytocompatibility of Ti6Al4V and Ti5Al2.5Fe alloys according to three surface treatments, using human fibroblasts and osteoblasts. Biomaterials 1996;17:929.
[19] Sauberlich S, Klee D, Richter EJ, Hocker H, Spiekermann H. Cell culture tests for assessing the tolerance of soft tissue to variously modified titanium surfaces. Clin Oral Implant Res 1999;10:379.
[20] Siegel RW. Creating nanophase materials. Sci Am 1996;275:42.
[21] Klabunde KJ, Strak J, Koper O, Mohs C, Park D, Decker S, Jiang Y, Lagadic I, Zhang D. Nanocrystals as stoichiometric reagents with unique surface chemistry. J Phys Chem 1996;100:12141.
[22] Webster TJ, Ergun C, Doremus RH, Siegel RW, Bizios R. Specific proteins mediate enhanced osteoblast adhesion on nanophase ceramics. J Biomed Mater Res 2000;51:475.
[23] Webster TJ, Schadler LS, Siegel RW, Bizios R. Mechanisms of enhanced osteoblast adhesion on nanophase alumina involve vitronectin. Tissue Eng 2001;7:291.